Oxygen reduction at negatively charged iron porphyrins heat-treated and bridged by alkaline-earth metal ions

Oxygen reduction at negatively charged iron porphyrins heat-treated and bridged by alkaline-earth metal ions

Takahiro Yamaguchi*[1], Kengo Tsukamoto, Osamu Ikeda**[1], Ryotaro Tanaka, Takayuki Kuwabara, Kohshin Takahashi

Faculty of Chemistry, Institute of Science and Engineering, Kanazawa university, Kakuma-machi, Kanazawa 920-1192, Japan

*corresponding author. Tel.: +81 76 234 4772; Fax: +81 76 234 4800.

**Corresponding author. Tel. +81 76 274 1357

E-mail address: t-yamagu@t.kanazawa-u.ac.jp (T. Yamaguchi), qqf549hd@themis.ocn.ne.jp (O. Ikeda).

[1] ISE member

ABSTRACT

An ordered network of tetrasodium tetra(4-sulphonatophenyl)porphyrin iron(III) chloride ($FeTPPS_4Na_4$), which exhibited a higher catalytic activity for oxygen reduction than Co and $Ir(CO)TPPS_4Na_4$, was fabricated by complexation with alkaline-earth metal ions. Heat treatment of these complexes enhanced their catalytic activity with the

highest performance observed with Ba^{2+}-$FeTPPS_4$. The onset potential for oxygen reduction (E_{onset}) was 720 mV vs. Ag|AgCl, which is almost the same as that for Pt-impregnated carbon black. The number of electrons, *n*, transferred during oxygen reduction at a Ba^{2+}-$FeTPPS_4$-coated electrode, as determined by rotating ring-disc experiments, was 3.9 and suggests that oxygen was reduced to water. A neutral solution of $FeTPPS_4Na_4$ was acidified by the addition of barium ion, and the elemental ratio Fe:S:Ba in the resulting Ba^{2+}-$FeTPPS_4$ complex was approximately 1:4:2.5. This suggests the formation of a highly ordered network with Fe sites bridged with barium ions in addition to the normal salt bridges between sulphonates. Catalytic oxidation reactions with nitric oxide and nitrite ion as the intermediate at the heat-treated Ba^{2+}-$FeTPPS_4$ indicate the formation of Fe(IV) and Fe(IV) π-cation radicals or Fe(V). The agreement between the potential of Fe(IV) π-cation radical formation and E_{onset} suggests that the redox cycle of the Fe(III)/Fe(IV) π-cation radical provides a sufficient driving force for the observed 4-electron reduction of oxygen at the heat-treated Ba^{2+}-$FeTPPS_4$ electrode.

Keywords:

Tetra(4-sulphonatophenyl)porphyrin iron(III)

Oxygen reduction

Barium salt

High valent iron

Face-to-face structure

1. Introduction

Catalysts for oxygen reduction are being actively pursued for practical applications in hydrogen–oxygen fuel cells. In particular, the development of inexpensive catalysts, or non-precious metal catalysts (NPMCs), to replace those incorporating metals such as platinum has become a matter of great urgency due to an anticipated exhaustion of noble metals. Various metal-containing macrocycles, or metallomacrocycles, have been studied as NPMC materials. Recently, cobalt-polypyrrole [1] and heat-treated cobalt porphyrin [2] have shown considerable promise.

In metallomacrocycles, the metal centre participates directly in the oxygen reduction mechanism. A face-to-face cobalt-porphyrin was developed by Collman et al. [3] that increases the number of electrons transferred to a coordinated oxygen molecule at the metal site such that a $4e^-$ reduction of oxygen to water occurs through O=O bond fission.

In addition to the above face-to-face configuration, which unites two porphyrin rings by covalent bond formation, a face-to-face iron-porphyrin, which utilises ionic bonds, has also been reported [4]. These face-to-face porphyrins have resulted in excellent catalytic activity for the $4e^-$ reduction of oxygen. Oxygen reduction at Co- and Fe-macrocycles is thought to occur through coordination of oxygen to Co(II) or Fe(II) and the formation of Co(III) or Fe(III) by a single electron transfer, namely a Co(II)/Co(III) or Fe(II)/Fe(III) redox mechanism. However, one of the authors (O. I.) [5] has indicated that this redox reaction did not necessarily control the oxygen reduction, especially in acidic solution. Bouwkamp-Wijinoltz et al. [6] suggested that oxygen reduction may occur through a Fe(II)/Fe(V) or Fe(IV) π-cation radical as in cytochrome P450 [7]. A new oxygen reduction mechanism has been proposed in the face-to-face cobalt porphyrin [8], in which the formation of a π-cation radical is a key factor in the coordination of oxygen to the metal site. Recently, a study reported that oxygen coordinates Fe(III) rather than Fe(II) to form an oxo dimer of Fe(IV) [9], although this study was conducted with a non-heme complex. The results cited above indicate that the formation of a high-valent metal may be important in oxygen reduction at metallomacrocycles.

Heat treatment has been shown effective in practical applications of metal macrocycles as catalysts for oxygen reduction since 1976 [10]. In addition, the current

study focuses on the use of highly ordered layer structures created with barium salts of organic multi-sulphonate compounds [11]. Oxygen reduction ability and the effects of heat treatment were evaluated for the alkaline-earth metal salt of tetra(4-sulphonatophenyl)porphyrin iron(III) ($FeTPPS_4$), which was the most promising compound amongst the Co, Ir(CO) and Fe complexes of H_2TPPS_4. A possible redox mechanism involving the Fe(III)/Fe(IV) π-cation radical or Fe(V) was demonstrated.

2. Experimental

2.1. Synthesis of metalloporphyrins

The metal-free sodium salt of tetra(4-sulphonatophenyl)porphyrin ($H_2TPPS_4Na_4 \cdot 12H_2O$; Strem) was used as the starting material. The sodium salt of tetra(4-sulphonatophenyl)porphyrin iron(III) chloride ($Fe(Cl)TPPS_4Na_4$) was synthesised by an ion-exchange reaction with a one-half-equivalent of $BaCl_2$ and $Fe(1/2SO_4)TPPS_4Na_4$. The latter was prepared according to a method by Fleisher et al. [12]. The sodium salt of tetra(4-sulphonatophenyl)porphyrin cobalt(III) chloride ($Co(Cl)TPPS_4Na_4$) was synthesised by a method similar to that of Hatano et al. [13], but

with $CoCl_2$ as a metalising agent. The sodium salt of tetra(4-sulphonatophenyl)porphyrin iridium(III) chloride was synthesised by refluxing $H_2TPPS_4Na_4$ with $Ir(CO)_3Cl$ (Strem) in dimethyl acetoamide for 15 h. The crude product was purified through a silica gel column and eluted with a mixed solvent of methanol/acetone (50/50 v/v). The iridium content and the IR spectrum suggested an actual composition of $Ir(CO)(Cl)TPPS_4Na_4 \cdot 12H_2O$.

2.2. Preparation of catalyst-coated electrodes

The coating of metalloporphyrin onto the electrode surface was fixed at 3×10^{-7} mol cm^{-2}. For example, 150 μL of 1 mM aqueous Fe, Co and $Ir(CO)TPPS_4Na_4$ was coated onto the centre portion (8 mm φ) of a glassy carbon (GC) plate (16 mm φ) and dried. Water-insoluble, alkaline-earth metal salts of the metalloporphyrin were coated onto the glassy carbon plate as a uniform colloidal solution. The colloidal solution was prepared primarily for $FeTPPS_4Na_4$ by an addition of 50 equivalents of 1 M alkaline-earth metal chloride to 1 mM of $FeTPPS_4Na_4$ or by an addition of 3 equivalents of 1 M alkaline-earth metal hydroxide to 1 mM $FeTPPS_4H_4$, which was obtained by passing 1 mM $FeTPPS_4Na_4$ through a H-form cation exchange resin. Coating amount of each

metalloporphyrin in mg cm^{-2} were 0.39, 0.39, 0.44, and 0.40 for Fe, Co, Ir(CO)$TPPS_4$ Na_4, and Ba^{2+}-$FeTPPS_4$ as an alkaline-earth metal salt of Fe $TPPS_4$ Na_4, respectively.

Heat treatment of the metalloporphyrin-coated glassy carbon consisted of baking for 10 min at 700°C in a quartz tube filled with ultrapure argon gas (Japan Fine Products, 99.9999%).

Steady-state voltammetric measurements were performed on a Pt/carbon black (Pt/CB)-loaded GC electrode (8 mm φ) that had been coated with a 5-μL dispersion of 20 wt% Pt/CB (Kawaken Fine Chemicals), which was made by adding 1.25 mg Pt/CB to 0.31 mL of a 5 wt% Nafion/alcohol solution, and dried. Rotating ring-disc voltammograms were acquired on Ba^{2+}-$FeTPPS_4$ and Ba^{2+}-$FeTPPS_4$/CB-loaded GC disc electrodes. The former electrode was prepared as following: a GC rod with a diameter of 6 mm and a length of 10 mm was used as the disc electrode. The amount of Ba^{2+}-$FeTPPS_4$ corresponding to 0.40 mg cm^{-2} was at first coated onto one of the circular faces of the rod and then heat-treated. The other end of the rod was connected to a Cu wire with Ag paste. The rod was carefully positioned in the RRDE mount using a low melting point Teflon resin. The latter electrode was prepared by coating a mixture of Ba^{2+}-$FeTPPS_4$ and CB (Vulcan XC-72) onto a GC disc electrode. Thus, CB corresponding to 40 wt% of solid materials was added to a colloidal solution of

Ba^{2+}-$FeTPPS_4$ and the solution was stirred for more than 6 hr by using a magnetic stirrer. The mixture of Ba^{2+}-$FeTPPS_4$ and CB was filtered out, and washed carefully with small amount of distilled water and then dried. The mixture was heat treated at 700°C for 10 min in ultra-pure Ar. and thereafter ultrasonically washed in 0.2 M $HClO_4$ and then with distilled water. The mixture dried at 60°C, 5 mg, was dispersed in 0.3 ml of 0.75 wt% Nafion/propanol solution, and its 30 μL was coated onto the disc electrode. The amount of Ba^{2+}-$FeTPPS_4$/CB on the disc (0.28 cm^2) was estimated to be 0.5mg.

2.3. Electrochemical measurements

Cyclic and steady-state voltammetries were performed in 0.2 M $HClO_4$ or 0.5 M H_2SO_4 using an inert electrode holder with open hole of 8 mm φ, in which the metalloporphyrin-coated glassy carbon plate was set, a potentiostat (Fuso, HECS 972), a potential sweeper (Fuso, HECS 980) and a recorder (Yokogawa, 3025). The reference electrode consisted of a Ag|AgCl electrode immersed in 3 M NaCl and a Pt plate was used as the counter electrode. Oxygen reduction experiments were carried out in an oxygen-saturated electrolytic solution. For control experiments, the removal of dissolved oxygen from the electrolytic solution was ensured by bubbling the solution

with ultrapure argon gas for 20 min. The electrochemical oxidation of nitric oxide (NO) was measured by adding a small amount of nitrite solution into the carefully deoxygenated electrolytic solution. Equilibrium drives the conversion of nitrite ion to nitric oxide under highly acidic conditions [14].

2.4. Rotating ring-disc electrode (RRDE) measurements

RRDE measurements were performed with a dual-potentiostat (Nikko Keisoku, DPGS-1), a function generator (Nikko Keisoku, NFG-3), a rotator (Nikko Keisoku, RRDE-1) and a controller (Nikko Keisoku, SC-5). Rotation speeds were changed from 500 to 3000 rpm. The reference electrode consisted of Ag|AgCl in 3 M NaCl and the ring electrode was composed of Pt. Before the measurement, the Pt ring electrode was cleaned by repeating a potential sweep at a rate of 10 mV s^{-1} between -150 mV and 1150 mV vs. Ag|AgCl in 0.2 M $HClO_4$. The ring potential was maintained at 1100 mV vs. Ag|AgCl to detect hydrogen peroxide. The oxygen-saturated electrolytic solution was prepared by bubbling pure oxygen gas for 20 min.

2.5. Thermal analyses

Thermal gravimetric analyses were carried out on a Rigaku TAS 100 thermal balance under an atmosphere of argon flowing at a rate of 20 mL min^{-1}. Heating rate was 10°C min^{-1}, and the heating was started from a room temperature and stopped at 800°C and 750°C for Ba^{2+}-$FeTPPS_4$ and $FeTPPS_4$, respectively.

2.6. Scanning electron microscopy (SEM) and elemental analysis

SEM micrographs were acquired on a Hitachi S-4500. Elemental analyses (C, O, S, Ba and Fe) of Ba^{2+}-$FeTPPS_4$ before and after heat treatment were made with an energy-dispersive X-ray (EDX) (Horiba EMAX-7000) and X-ray fluorescence (XRF) (Horiba, XGT-7000V) spectrometers. Since C and O are not quantifiable with XRF, the mass percentages obtained from EDX were assumed as known values against which the other elemental components were measured.

3. Results and discussion

3.1. Oxygen reduction at heat-treated metalloporphyrins of H_2TPPS_4

The effects of the metal centre on oxygen reduction were studied on heat-treated Fe, Co and Ir(CO)$TPPS_4Na_4$. Fig. 1A shows cyclic voltammograms obtained on electrodes coated with heat-treated $FeTPPS_4$ in 0.5 M H_2SO_4 saturated with (a) argon and (b) oxygen. Fig. 1B shows cyclic voltammograms obtained at the 20 wt% Pt/CB electrode in 0.5 M H_2SO_4 saturated with (a) argon and (b) oxygen. The ability to reduce oxygen, as indicated by the reduction peak potential (E_{pc}), decreased as Pt/CB (540 mV) > $FeTPPS_4$ (450 mV) > $CoTPPS_4$ (440 mV) > Ir(CO)$TPPS_4$ (350 mV vs. Ag|AgCl). Under these experimental conditions, $FeTPPS_4$ and $CoTPPS_4$ performed similarly, but low catalytic activity was observed with Ir(CO)$TPPS_4$. This may be a result of structural differences in Ir(CO)$TPPS_4$ due to the presence of CO, a strong ligand. The present study therefore focuses on $FeTPPS_4$, which showed the highest degree of oxygen reduction amongst the metalloporphyrins evaluated.

3.2. Oxygen reduction at heat-treated $FeTPPS_4$ bridged by alkaline-earth metal ions

The bridging the $FeTPPS_4Na_4$ molecules with divalent alkaline-earth metal ions, and its effects on oxygen reduction activity, was studied. The degree of bridging was

estimated by the formation of precipitate. The results are shown in Fig. 2 and are summarised in Table 1. Oxygen reduction deceased, as determined by E_{pc}, as Ba^{2+} > Sr^{2+} > Ca^{2+} > None (Na^{+}) > Mg^{2+}. This order was in good agreement with ionic size and suggests that counter cations control the aggregate structure of $FeTPPS_4$.

Fig. 3 shows steady-state voltammograms for oxygen reduction at heat-treated $FeTPPS_4Na_4$, its barium salt (Ba^{2+}-$FeTPPS_4$) and the Pt/CB electrode. The degree of oxygen reduction was higher at the Ba^{2+}-$FeTPPS_4$-coated electrode, and the onset potential was nearly the same as that of Pt/CB.

3.3. RRDE measurements

Fig. 4 shows rotating ring-disc voltammograms for oxygen reduction at pure Ba^{2+}-$FeTPPS_4$ and at a Ba^{2+}-$FeTPPS_4$/CB-coated electrode that had been heat-treated at 700^{o}C for 10 min. The former electrode sometimes showed an exfoliation of Ba^{2+}-$FeTPPS_4$ film during rotation of RRDE. Therefore, the latter electrode was examined to improve the contact with a base GC disc electrode. Both catalysts showed small ring currents around 100 mV vs. Ag|AgCl, implying scarce formation of hydrogen peroxide upon oxygen reduction. The ring and disc current ratios (I_R/I_D) were 0.0054

and 0.0113 for pure Ba^{2+}-$FeTPPS_4$ and Ba^{2+}-$FeTPPS_4$/CB electrodes, respectively. Owing to differences in surface roughness, the actual collection efficiency (N) was estimated for both catalysts using the redox of hexacyanoferrate (III)/(II), and was 0.30 for Ba^{2+}-$FeTPPS_4$ and 0.32 for Ba^{2+}-$FeTPPS_4$/CB. From these data, the number of electrons transferred during oxygen reduction may be calculated by $n = 4I_D/[I_D + (I_R/N)]$ [15] and was 3.9 for both catalysts. This result demonstrates a 4-electron ($4e^-$) reduction of oxygen at the heat-treated Ba^{2+}-$FeTPPS_4$ electrode.

Further, the slope of Koutecky-Levich plot shown in inset of Fig. 4 suggested n=3.8.

3.4. Estimation of the structure of Ba^{2+}-$FeTPPS_4$

The ability of Ba^{2+}-$FeTPPS_4$ to efficiently reduce oxygen may be due in part to its unique morphology. SEM micrographs in Fig. 5 show $FeTPPS_4Na_4$ and Ba^{2+}-$FeTPPS_4$ before and after heat treatment. Ba^{2+}-$FeTPPS_4$ exhibits a unique fibrile mesh structure, both before and after heat treatment, that was not observed for the strontium (Sr^{2+}-$FeTPPS_4$), calcium (Ca^{2+}-$FeTPPS_4$) or magnesium salts (Mg^{2+}-$FeTPPS_4$), which all showed morphological characteristics similar to those of $FeTPPS_4Na_4$. The barium salts of organic sulphonates adopt an ordered structure in the solid state that changes

with the number of sulphonate groups in the molecule [11]. Therefore, a highly ordered, three-dimensional structure can be expected with the barium salt of $FeTPPS_4Na_4$ with four sulphonate groups.

The pH of the $FeTPPS_4Na_4$ was carefully monitored during titration with $BaCl_2$. As shown in Table 2, the initially neutral solution became acidic after the addition of $BaCl_2$. For each of the salts evaluated, the degree of pH change decreased in the following order: $Ba^{2+} > Sr^{2+} > Ca^{2+} > Mg^{2+}$. Since both solutions of $FeTPPS_4Na_4$ and $BaCl_2$ were originally neutral, this pH change indicates a reaction between $FeTPPS_4Na_4$ and $BaCl_2$. The most probable reaction is illustrated in Fig. 6, whereby at neutral pH, Ba^{2+} reacts with a hydroxide-bearing intermediate formed in equilibrium with the monomeric and dimeric forms of $FeTPPS_4Na_4$ [12]. No changes were observed at extreme pH (Table 2) due to the disappearance of small amounts of H^+, which had initially been present, at high concentrations of H^+ or OH^-. However, the absence of any precipitate under highly acidic conditions suggests that the monomeric form of $FeTPPS_4Na_4$, in which the Fe site is coordinated with water, does not react with Ba^{2+}. During the titration of $FeTPPS_4Na_4$ by $BaCl_2$, a steep rise in pH was observed at the onset of titration. This suggests that the rate of bridge formation between two Fe sites by Ba^{2+} is higher than that of salt formation between the sulphonate groups by Ba^{2+}, or that both reactions

proceed simultaneously. The speculated structure of the barium salt of $FeTPPS_4Na_4$ (Ba^{2+}-$FeTPPS_4$) is shown in Fig. 7. This structure contains a face-to-face site inside the network, and is strongly correlated with the ability of Ba^{2+}-$FeTPPS_4$ to reduce oxygen.

The distance between two Fe sites in a face-to-face structure of Ba^{2+}-$FeTPPS_4$ was roughly estimated by using ionic radii of Fe^{3+}(0.07 nm) and Ba^{2+}(0.15 nm) [16] to be 0.44 nm, and the formed cavity is able to accommodate oxygen molecule (0.34 nm, kinetic diameter) and peroxide ion (0.36 nm, thermochemical diameter) [17]. The value of 0.44 nm was very close to ~0.4 nm in the co-facial cobalt porphyrin that showed a $4e^-$ reduction of oxygen [3].

3.5. Compositional changes of Ba^{2+}-$FeTPPS_4$ as a result of heat treatment

Heat-induced morphological changes in Ba^{2+}-$FeTPPS_4$ were not significant as shown in Fig. 5. Thermal gravimetric analyses of $FeTPPS_4Na_4$ and Ba^{2+}-$FeTPPS_4$ (Fig. 8) revealed a higher thermal stability for Ba^{2+}-$FeTPPS_4$ with no loss of waters of crystallisation around 100–200^oC. The main decrease in mass begins at 530^oC in Ba^{2+}-$FeTPPS_4$ and 420^oC in $FeTPPS_4Na_4$. The higher thermal stability and maintenance of molar ratio after the main decomposition of Ba^{2+}-$FeTPPS_4$ suggests a dense structure

formed by multiple bridges.

The results of XRF and EDX analyses for elemental composition, acquired at two or three different points on powdered Ba^{2+}-$FeTPPS_4$ samples, are summarised in Table 3. The results for unheated Ba^{2+}-$FeTPPS_4$ are in good agreement with theoretical values based on the estimated molecular formula, $C_{44}H_{24}N_4O_{13}S_4Fe_1Ba_{2.5}$. The results following heat treatment showed an increase in the mass percent of carbon, but the basic molar ratio amongst S, Fe and Ba remained roughly the same as theory would predict. This suggests that whilst the face-to-face structure shown in Fig. 6 was maintained, the relatively unstable edges of the network structure was decomposed and carbonised during heat treatment. This carbonisation may also cause an increase in the electrical conductivity of the catalyst. The specific resistance of unheated and heat-treated Ba^{2+}-$FeTPPS_4$ changes from that of an insulator ($\rho > 6 \times 10^8$ Ω cm) to that of a conductor ($\rho > 2 \times 10^2$ Ω cm). The EDX spectra contained evidence of significant Cl after acid washing of the heat-treated Ba^{2+}-$FeTPPS_4$, but not for the dried samples of unheated and heat-treated Ba^{2+}-$FeTPPS_4$. Since the heat-treated Ba^{2+}-$FeTPPS_4$ was washed in 0.2 M $HClO_4$ and rinsed with water until the filtrate was neutral, the presence of Cl as ClO_4^- suggests the presence of occlusions in the film. However, accepting this possibility is difficult because the net charge of Ba^{2+}-$FeTPPS_4$ is initially zero. One

possibility is the formation of high-valent Fe (Fe(IV) or Fe(V)) by contact with dissolved oxygen. Bouwkamp-Wijnoltz et al. [18] confirmed the presence of high-valent Fe(IV) in heat-treated FeTPP (tetraphenyl porphyrin) by Mössbauer spectroscopy.

3.6. Redox of the Fe site and oxygen reduction mechanisms

A clear redox reaction is not evident in the cyclic voltammogram of the heat-treated Ba^{2+}-$FeTPPS_4$ shown in Fig. 2. Since heat-treated metallomacrocycles do not usually exhibit a clear redox behaviour [19], an indirect method, relying on the oxidation of nitric oxide, was used to detect the redox activity of heat-treated Ba^{2+}-$FeTPPS_4$ or the formation of high-valency iron species. Oxo ferryl iron-porphyrin ($O=Fe^{IV}$-P) catalyses the $1e^-$ oxidation of nitric oxide, and the oxo ferryl iron-porphyrin π-cation radical ($O=Fe^{IV}$-$P^{+\cdot}$ or $O=Fe^{V}$-P) catalyses a $2e^-$ oxidation of the resulting nitrite to nitrate [20]. Fig. 9 shows the electrochemical oxidation of nitrite at heat-treated Ba^{2+}-$FeTPPS_4$ in 0.2 M $HClO_4$. Under these acidic conditions, all of the added nitrite was converted to nitric oxide due in an equilibrium reaction [14] and the oxidation wave around 0.5 V–0.6 V corresponds to the $1e^-$ oxidation of nitric oxide to nitrosonium ion (NO^+) by $O=Fe^{IV}$-P.

The second wave around 0.7 V corresponds to the $2e^-$ oxidation of nitrite, which was formed by the reaction of NO^+ with surface water, to nitrate. These assignments were confirmed by the absence of corresponding waves at a bare glassy carbon electrode.

Bouwkamp-Wijnoltz et al. [6] suggested an oxygen reduction mechanism at heat-treated FeTPPCl in which the oxygen, which was initially coordinated to Fe(II), forms a hydroperoxide complex (Fe(III)OOH) and is reduced to Fe(II) through an oxo ferryl intermediate (O=Fe(IV)). This mechanism is similar to that of cytochrome P450 [7]. Thereafter, Bouwkamp-Wijnoltz et al. [18] verified the presence of all iron oxidation states (Fe(I), Fe(II), Fe(III) and Fe(IV)) in dry heat-treated FeTPPCl by Mössbauer spectroscopy, and provided evidence for increasing amount of Fe(IV) in an aqueous solution of 0.5 M H_2SO_4.

One of the authors [5] has suggested, based on spectroelectrochemical experiments, that oxygen reduction at $FeTPPS_4$ in a polypyrrole matrix in acidic solutions proceeds with Fe(III) but not with Fe(II). Recently, a study reported that oxygen does not coordinate Fe(II) but rather Fe(III) to form an oxo dimer of Fe(IV) [9]. The iron complex evaluated in the aforementioned study was not a porphyrin, but did contain a N_4 chelation site. The above results suggest that oxygen is able to coordinate with Fe(III) under certain conditions. As shown in Fig. 9, the onset potential for oxygen

reduction is in fair agreement with that of Fe(IV) π-cation radical formation, whereby the oxidation of nitrite begins. Therefore, we propose the oxygen reduction mechanism shown in Fig. 10, which assumes the initial coordination of oxygen to Fe(III) or two adjacent nitrogen atoms, an intermediate peroxide, and finally the formation of a Fe(IV) π-cation radical. The presence of peroxide complex as an intermediate may be explained by small oxidation currents around 500 mV vs. Ag|AgCl which were observed at the reverse scan of the cyclic voltammogram in Fig. 2. This peroxide intermediate seems to be stable only on the cyclic voltammetric scale at a room temperature. The proposed mechanism features a face-to-face structure that allows oxygen to react with two nitrogen atoms in the vertical position. The above discussions indicate that the formation of high-valent metal may be important in oxygen reduction at metalloporphyrins. Raman spectroscopy will be useful for the direct confirmation of high-valent metal species or peroxide complex as an intermediate.

4. Conclusions

Three heat-treated metal complexes of tetra(4-sulphonatophenyl)porphyrin, $FeTPPS_4Na_4$, $CoTPPS_4Na_4$ and $Ir(CO)TPPS_4Na_4$ were evaluated as catalysts for oxygen

reduction. The highest degree of oxygen reduction was observed with $FeTPPS_4Na_4$, which adopted an ordered structure through the formation of alkaline-earth metal ion bridges. The ability of metal salts of $FeTPPS_4Na_4$ to reduce oxygen increased with the size of the bridging ion; the highest performing compound was the barium salt (Ba^{2+}-$FeTPPS_4$). Steady-state and rotating ring disc voltammograms at a heat-treated Ba^{2+}-$FeTPPS_4$-coated electrode showed almost the same onset potential for oxygen reduction and the same capability for reducing oxygen to water as those of platinum. Titration of neutral aqueous $FeTPPS_4Na_4$ with barium ion lowered the pH of the solution. This result suggests the formation of barium ion bridges between Fe sites to create a face-to-face structure, in addition to the bridging between sulphonate groups. Thermogravimetric and elemental analyses indicated that this face-to-face structure was stable during heat treatment in argon and in acidic solution. The macromolecular conformation and the distance between the two faces (porphyrin rings) were controlling factors in oxygen coordination. Bridge formation with barium ion provides adequate space for oxygen coordination. The vertical conformation of nitrogen atoms adjacent to Fe(III) may allow easy coordination of oxygen and the formation of high valent iron species.

Acknowledgements

The authors would like to thank Drs. Makoto Ohishi and Ken-ichi Watanabe in the HORIBA Application Center for their valuable technical support during EDX and XRF analyses.

References

[1] R. Bashyam, P. Zelenay, Nature 443 (2006) 63.

[2] P. Bagdanoff, I. Herrmann, M. Hilgendorf, I. Dorbandt, S. Fiechter, H. Tributsch, J. New Mater. Electrochem. Syst. 7 (2004) 85.

[3] J. P. Collman, P. Danisevich, Y. Konai, M. Marrocco, C. Koval, F. C. Anson, J. Am. Chem. Soc. 102 (1980) 6027.

[4] T. Sawaguchi, T. Matsue, K. Itaya, I. Uchida, Electrochim. Acta 36 (1991) 703.

[5] O. Ikeda, K. Okabayashi, N. Yoshida, H. Tamura, J. Electroanal. Chem. 191 (1985) 157.

[6] A. L. Bouwkamp-Wijnoltz, W. Vissher, J. A. R. van Been, Electrochim. Acta 43 (1998) 3141.

[7] I. Schlichting, J. Berendzen, K. Chu, A. M. Stock, S. A. Maves, D. E. Benson, R. M. Sweet, D. Ringe, G. A. Petsko, S. G. Sliger, Science 287 (2000) 1615.

[8] Y. Le Mest, C. Inisan, A. Laouénan, M. L'Her, J. Talarmin, M. El Khalifa, J.-I. Saillard, J. Am. Chem. Soc. 119 (1997) 6095.

[9] A. Ghosh, F. T. de Oliveira, T. Yano, T. Nishioka, E. S. Beach, I. Kinoshita, E. Münck, A. D. Ryabov, C. P. Horwitz, T. J. Collins, J. Amer. Chem. Soc. 127 (2005) 2505.

[10] H. Yahnke, M. Schönborn, Z. Zimmerman, Fortschr. Chem. Forsch., 61 (1976) 133.

[11] A. P. Côté, G. K. H. Shimizu, Coord. Chem. Rev. 245 (2003) 49.

[12] E. B. Fleisher, J. M. Palmer, T. S. Srivastava, A. Chatterjee, J. Am. Chem. Soc. 93 (1971) 3162.

[13] K. Hatano, K. Usui, Y. Ishida, Bull. Chem. Soc. Jpn. 54 (1981) 413.

[14] E. Weeg-Aerssens, J. M. Tiedje and T. Averill, J. Am. Chem. Soc. 110 (1990) 685.

[15] R. Kothandaraman, V. Nallathambi, K. Artyushkova, S. C. Barton, Appl. Catal., B 92 (2009) 209.

[16] R. D. Shannon, Acta Crystallogr. Sect. A, 32 (1969) 751.

[17] T. C. Weddington, Adv. Inorg. Chem. Radiochem., 1 (1959) 180.

[18] A. L. Bouwkamp-Wijnoltz, W. Vissher, J. A. R. van Been, E. Beollaard, A. M. van der Kraan, S. C. Tang, J. Phys. Chem. B 106 (2002) 12993.

[19] S. Lj. Gojkovic, S. Gupta, R. F. Savinell, J. Electrochem. Soc. 145 (1998) 3493.

[20] J. Lei, N. S. Trofimova, O. Ikeda, Chem. Lett. 32 (2003) 610.

Fig. 1. Cyclic voltammograms at (A) heat-treated $FeTPPS_4Na_4$/GC and (B) Nafion-coated 20 wt% Pt/CB in (a) Ar and (b) O_2-saturated 0.5 M H_2SO_4. Potential sweep rate: 10 mV s^{-1}; geometric electrode surface area: 0.50 cm^2.

Fig. 2. Cyclic voltammograms of oxygen reduction at heat-treated complexes of $FeTPPS_4$ containing different alkaline-earth metals in an O_2-saturated 0.2 M $HClO_4$ solution. Potential sweep rate: 10 mV s^{-1}; geometric electrode surface area: 0.50 cm^2.

Fig. 3. Steady-state voltammograms of oxygen reduction at different catalyst electrodes in O_2-saturated 0.2 M $HClO_4$. None = heat-treated $FeTPPS_4Na_4$; Ba^{2+} = heat-treated Ba^{2+}-$FeTPPS_4$; Pt/CB = 20 wt% Pt on CB. Geometric electrode surface area: 0.50 cm^2.

Fig. 4. Rotating ring-disc voltammograms at (a) heat-treated Ba^{2+}-$FeTPPS_4$ and (b) Ba^{2+}-$FeTPPS_4$/CB-loaded disc electrodes in O_2-saturated 0.2 M $HClO_4$. Potential sweep rate at disc: 10 mV s^{-1}; ring potential: 1.1 V vs. Ag|AgCl; rotation rate: 2000 rpm. The inset shows a Koutecky-Levich (I_D^{-1} versus $\omega^{-1/2}$) at 0.1 V vs. Ag|AgCl .for Ba^{2+}-$FeTPPS_4$/CB-loaded disc electrode.

Fig. 5. SEM micrographs of (A) $FeTPPS_4Na_4$ and (B) Ba^{2+}-$FeTPPS_4$ on GC before and after heat treatment.

Fig. 6. Hypothesised reaction between Ba^{2+} and $FeTPPS_4$ showing the production of hydrogen ions.

Fig. 7. Speculated structure of Ba^{2+}-$FeTPPS_4$ before and after heat treatment.

Fig. 8. Thermograms showing the degradation of (a) $FeTPPS_4Na_4$ and (b) Ba^{2+}-$FeTPPS_4$.

Fig. 9. Cyclic voltammograms at heat-treated Ba^{2+}-$FeTPPS_4$ in deoxygenated 0.2 M $HClO_4$ with and without 1 mM $NaNO_2$. Potential sweep rate: 10 mV s^{-1}. NO_2^- is completely converted to NO due to the equilibrium reaction. The dotted line indicates E_{onset}, the onset potential of oxygen reduction in 0.2 M $HClO_4$ saturated with O_2.

Fig. 10. Proposed reaction mechanism for the four-electron reduction of oxygen at heat-treated Ba^{2+}-$FeTPPS_4$ on GC.

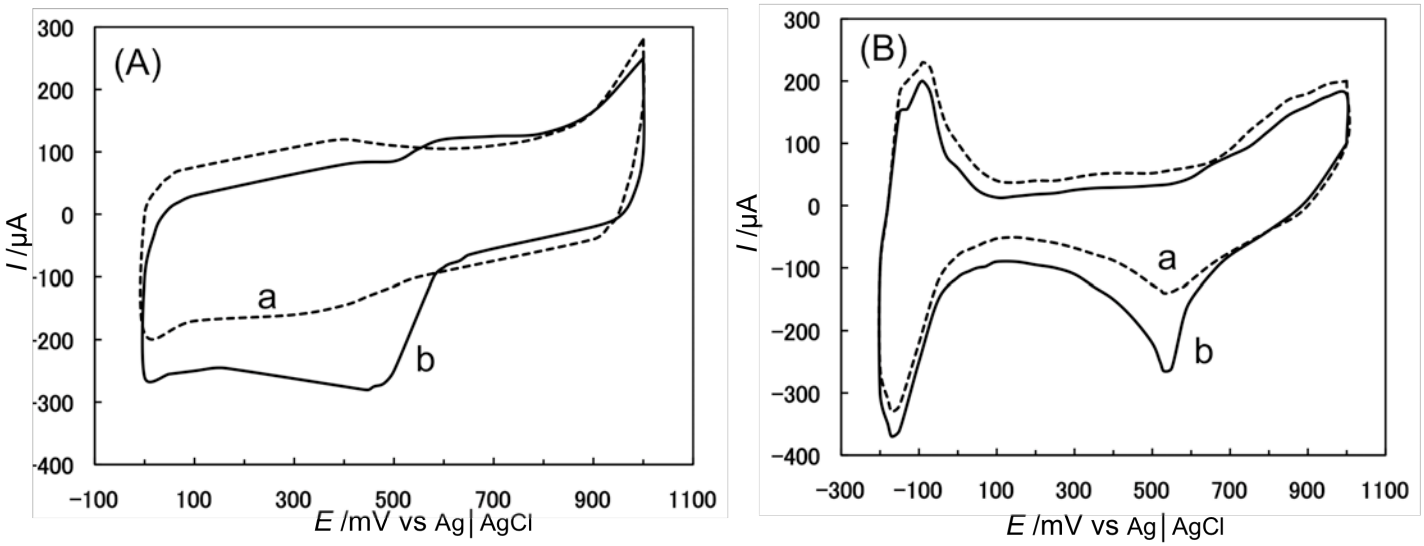

Fig. 1. Cyclic voltammograms at (A) heat-treated $FeTPPS_4Na_4$/GC and (B) Nafion-coated 20 wt% Pt/CB in (a) Ar and (b) O_2-saturated 0.5 M H_2SO_4. Potential sweep rate: 10 mV s^{-1}; geometric electrode surface area: 0.50 cm^2.

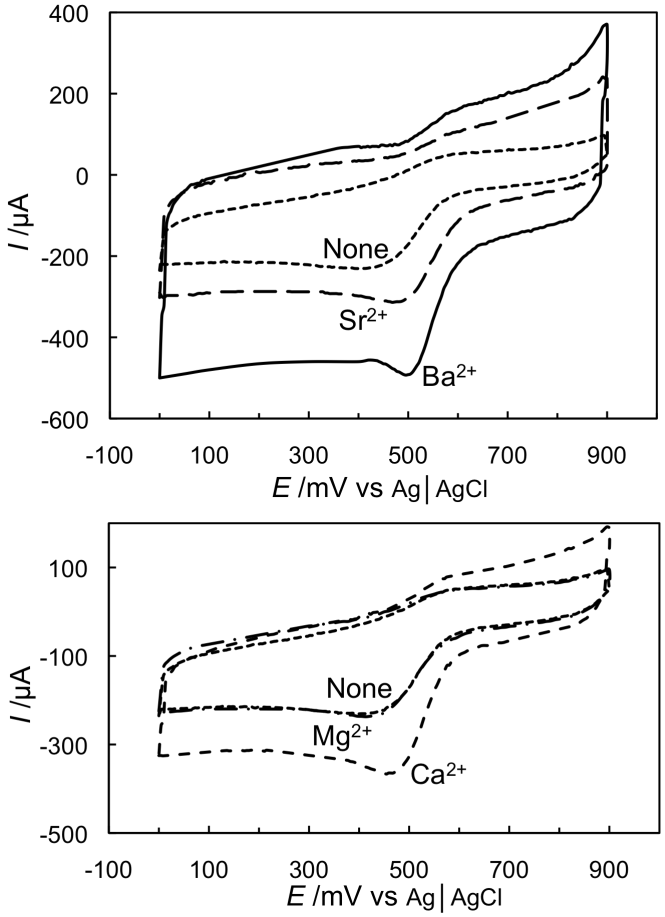

Fig. 2. Cyclic voltammograms of oxygen reduction at heat-treated complexes of $FeTPPS_4$ containing different alkaline-earth metals in an O_2-saturated 0.2 M $HClO_4$ solution. Potential sweep rate: 10 mV s^{-1}; geometric electrode surface area: 0.50 cm^2.

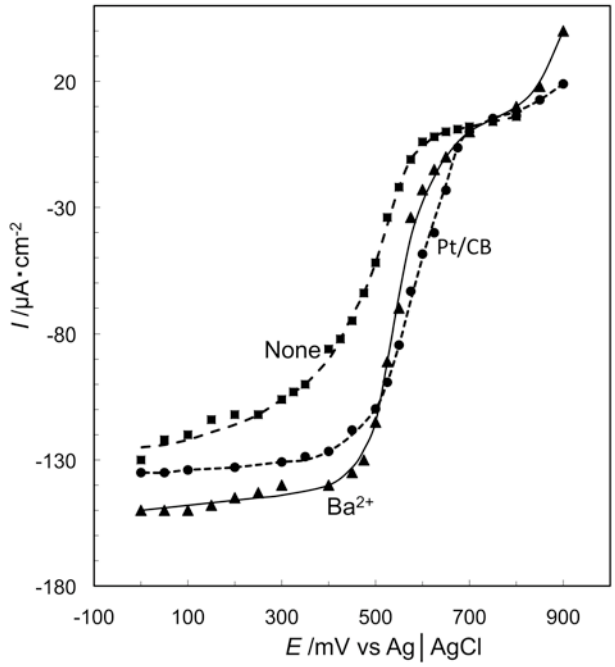

Fig. 3. Steady-state voltammograms of oxygen reduction at different catalyst electrodes in O_2-saturated 0.2 M $HClO_4$. None = heat-treated $FeTPPS_4Na_4$; Ba^{2+} = heat-treated Ba^{2+}-$FeTPPS_4$; Pt/CB = 20 wt% Pt on CB. Geometric electrode surface area: 0.50 cm^2.

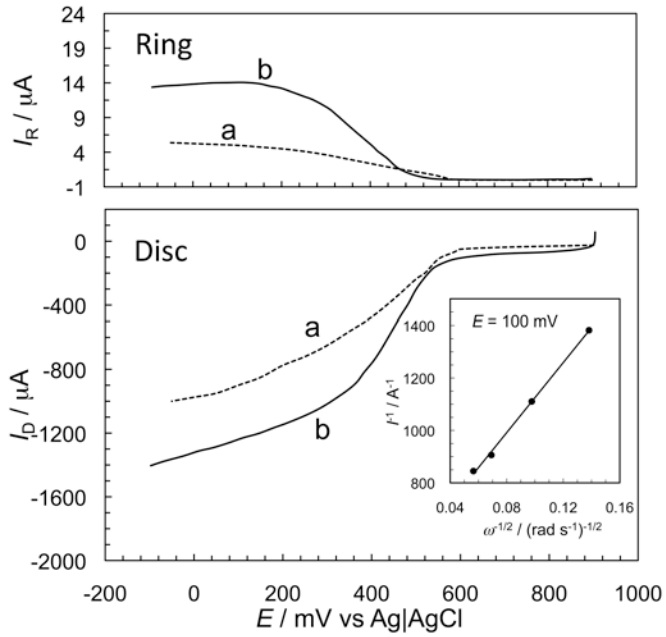

Fig. 4. Rotating ring-disc voltammograms at (a) heat-treated Ba^{2+}-$FeTPPS_4$ and (b) Ba^{2+}-$FeTPPS_4$/CB-loaded disc electrodes in O_2-saturated 0.2 M $HClO_4$. Potential sweep rate at disc: 10 mV s^{-1}; ring potential: 1.1 V vs. Ag|AgCl; rotation rate: 2000 rpm. The inset shows a Koutecky-Levich (I_D^{-1} versus $\omega^{-1/2}$) at 0.1 V vs. Ag|AgCl .for Ba^{2+}-$FeTPPS_4$/CB-loaded disc electrode.

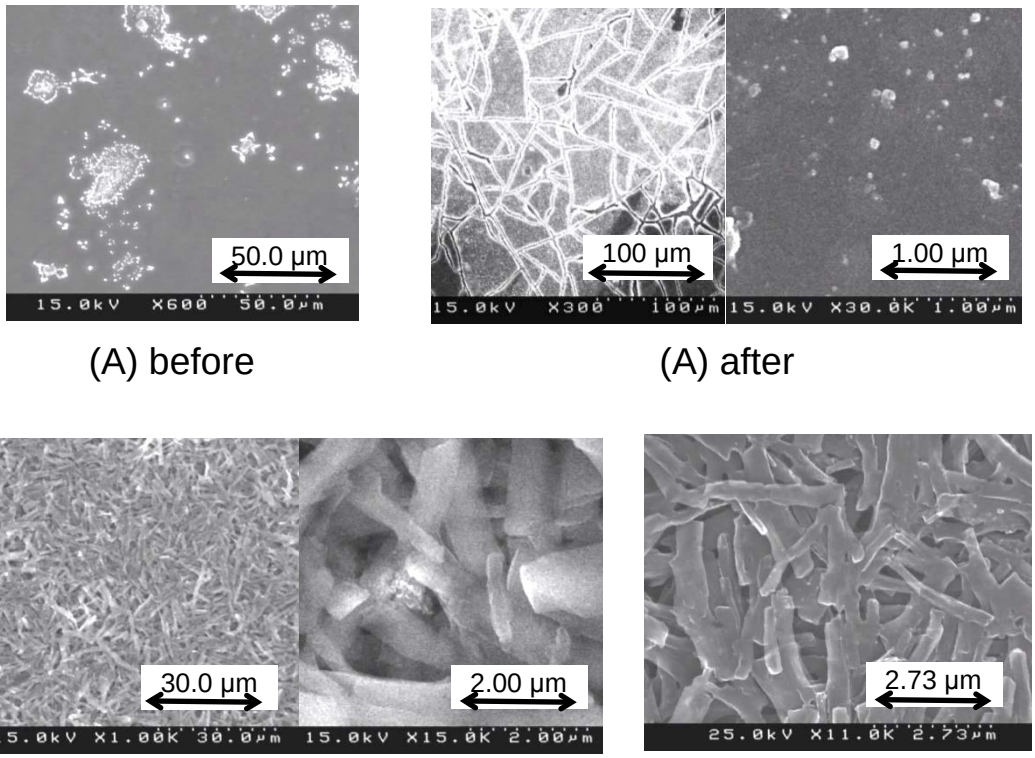

Fig. 5. SEM micrographs of (A) $FeTPPS_4Na_4$ and (B) Ba^{2+}-$FeTPPS_4$ on GC before and after heat treatment.

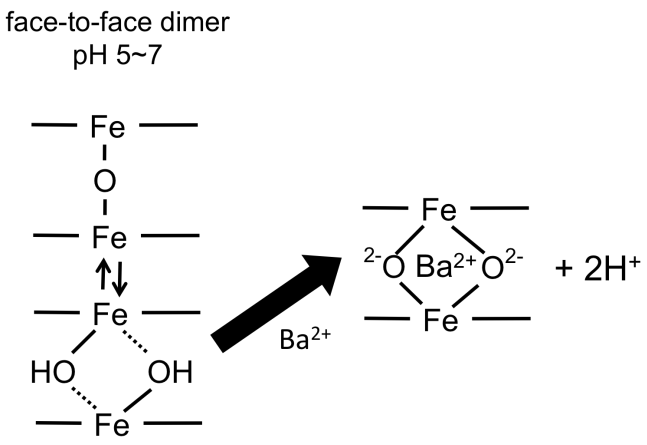

Fig. 6. Hypothesised reaction between Ba^{2+} and $FeTPPS_4$ showing the production of hydrogen ions.

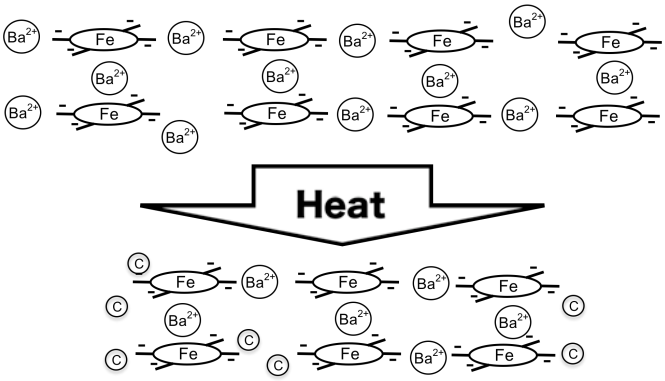

Fig. 7. Speculated structure of Ba^{2+}-$FeTPPS_4$ before and after heat treatment.

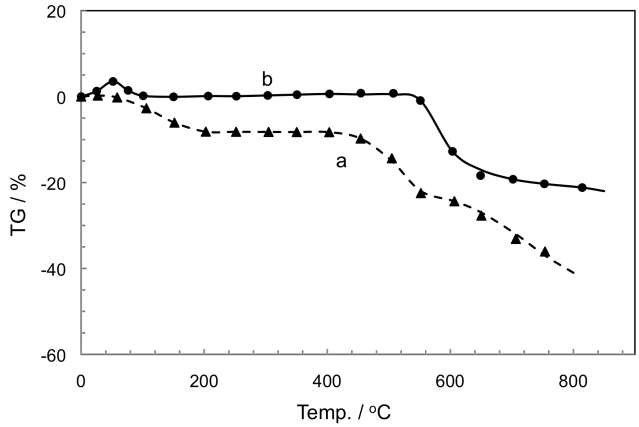

Fig. 8. Thermograms showing the degradation of (a) $FeTPPS_4Na_4$ and (b) Ba^{2+}-$FeTPPS_4$.

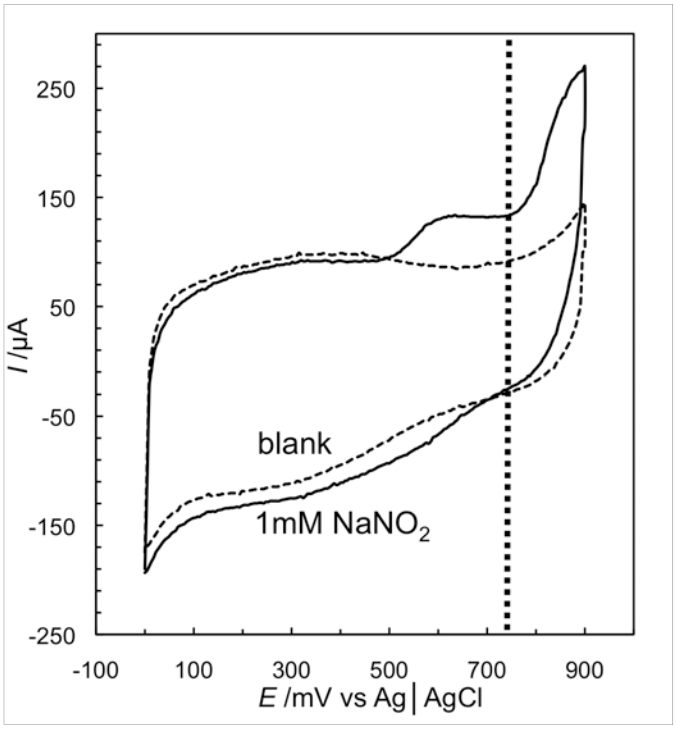

Fig. 9. Cyclic voltammograms at heat-treated Ba^{2+}-$FeTPPS_4$ in deoxygenated 0.2 M $HClO_4$ with and without 1 mM $NaNO_2$. Potential sweep rate: 10 mV s^{-1}. NO_2^- is completely converted to NO due to the equilibrium reaction. The dotted line indicates E_{onset}, the onset potential of oxygen reduction in 0.2 M $HClO_4$ saturated with O_2.

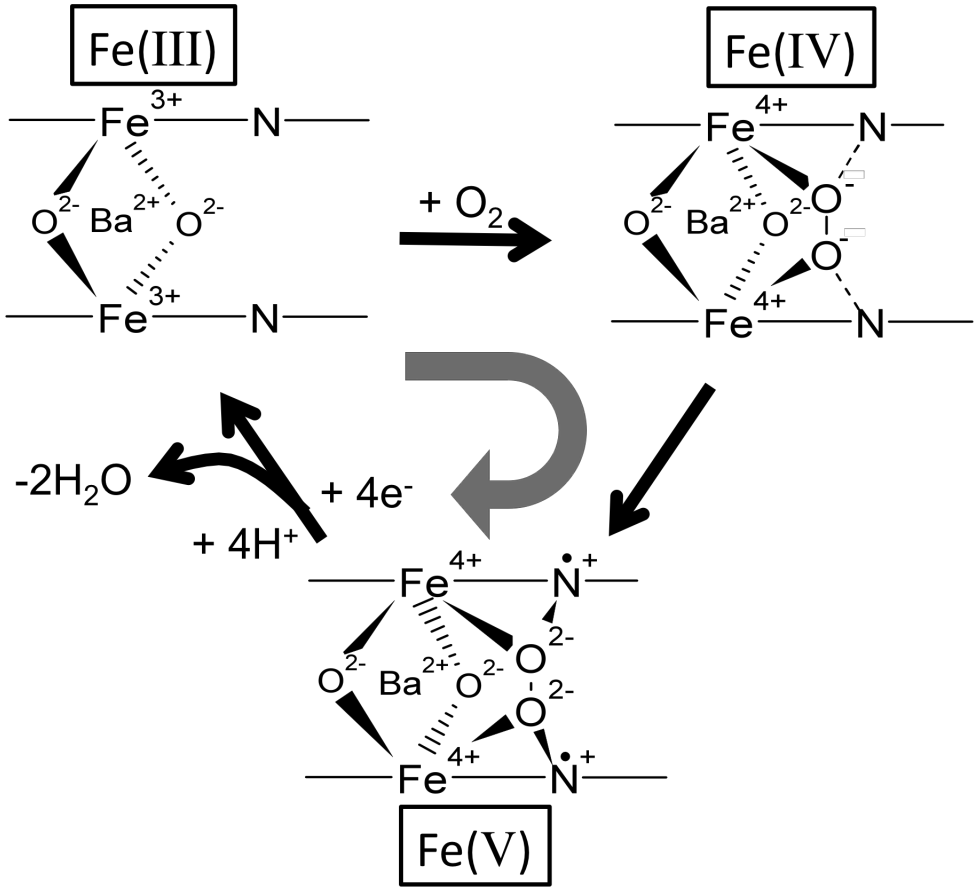

Fig. 10. Proposed reaction mechanism for the four-electron reduction of oxygen at heat-treated Ba^{2+}-$FeTPPS_4$ on GC.

Table 1

Cathodic peak potentials for oxygen reduction at various heat-treated $MTPPS_4$-coated electrodes.

$MTPPS_4$	E_{pc}/mV vs. Ag|AgCl
$FeTPPS_4$	450
$CoTPPS_4$	440
$Ir(CO)TPPS_4$	350

Table 2
The pH change induced by the addition of 100 equivalents $BaCl_2$ to 1 mM $FeTPPS_4$ and the cathodic peak potential for oxygen reduction at the heat-treated Ba^{2+}-$FeTPPS_4$ electrode.

Initial pH	Final pH	State of precipitate*	E_{pc}/mV vs. AglAgCl
2.5	2.5	×	400
5.5	3.6	○	470
7	5.5	◎	470
12	12	◎	420

*×, ○ and ◎ refer to none, medium and full precipitation, respectively.

Table 3
Elemental analyses by XRF and EDX for unheated and heat-treated Ba^{2+}-$FeTPPS_4$.

	EDX						XRF				
	C	O	S	Fe	Ba	Cl	C	O	S	Fe	Ba
Unheated Ba^{2+}-$FeTPPS_4$											
Observed											
Mass %	44.0	17.0	10.2	4.5	24.3	–	44*	17*	9.5	4.2	25.3
Molar ratio	45.9	13.3	4.0	1.0	2.2	–	(48.5)	(14.0)	4.0	1.0	2.4
Theoretical**											
Mass %	41.8	16.5	10.2	4.4	27.2	–	same as in EDX				
Molar ratio	44	13	4	1	2.5	–	same as in EDX				
Heat-treated Ba^{2+}-$FeTPPS_4$											
Observed											
Mass %	50.0	13.0	8.7	4.5	23.4	–	50*	13*	8.6	4.0	24.3
Molar ratio	52.0	10.1	3.5	1.0	2.1	–	(58.0)	(11.4)	3.8	1.0	2.5
0.2 M $HClO_4$ washing after heat treatment											
Observed											
Mass %	56.9	13.5	8.4	3.6	17.2	0.5	57*	13*	8.1	3.3	18.7
Molar ratio	73.2	13.0	4.0	1.0	1.9	0.2	81.5	13.9	4.3	1.0	2.3

Molar ratio was calculated by assuming Fe = 1 mole.

*The data for C and O were acquired by EDX analyses since XRF is unsuitable for these elements.

** Estimated molecular formula for unheated Ba^{2+}-$FeTPPS_4$ was $C_{44}H_{24}N_4O_{13}S_4Fe_1Ba_{2.5}$.